Available online at www.sciencedirect.com
ScienceDirect
Trans. Nonferrous Met. Soc. China 22(2012) 1118−1122
Transactions of Nonferrous Metals Society of China
www.tnmsc.cn

Effects of Cr_3C_2 content and wheel speed on amorphization behavior of melt-spun $SmCo_{7-x}(Cr_3C_2)_x$ alloys

LI Li-ya, YI Jian-hong, LI Ai-kun, PENG Yuan-dong, XIA Qing-lin

State Key Laboratory of Powder Metallurgy, Central South University, Changsha 410083, China

Received 18 May 2011; accepted 24 October 2011

Abstract: The effects of the Cr_3C_2 content and wheel speed on the amorphization behavior of the melt-spun $SmCo_{7-x}(Cr_3C_2)_x$ (x=0.10−0.25) alloys were studied systematically by X-ray diffraction analysis (XRD), differential scanning calorimetry (DSC) and magnetic measurements. The ribbon melt-spun at lower wheel speed (20 m/s) has composite structure composed of mostly $SmCo_7$ and a small amount of $Sm_2Co_{17}R$. The grain size of $SmCo_7$ phase decreases with the increase of Cr_3C_2 content. With the increase of wheel speed, the XRD peaks become lower and accompanied with a broad increase in backgrounds, indicating a considerable decrease in the grain size of the $SmCo_7$ phase. When the wheel speed increases to 40 m/s, $SmCo_{7-x}(Cr_3C_2)_x$ alloys can be obtained in the amorphous state for $0.15 \le x \le 0.25$ with intrinsic coercive H_{ci} of 0.004−0.007 T. The DSC analysis reveals that $SmCo_7$ phase firstly precipitates from the amorphous matrix at 650 °C, followed by the crystallization of Sm_2Co_{17} phase at 770 °C.
Key words: $SmCo_7$-type permanent magnets; Cr_3C_2; melt spinning; amorphization; hysteresis loops

1 Introduction

Permanent magnet materials capable of operating at elevated temperatures are needed for advanced power systems [1]. Most attention has been paid to the $SmCo_7$-type magnets because of their large coercivity and high Curie temperature [2]. Powder metallurgy method has been used successfully to fabricate $Sm(Co,Fe,Cu,Zr)_7$ bulk magnets with a coercivity of 1 T at 500 °C [3]. The microstructure of the sintered $SmCo_7$-type magnets consists of $Sm_2Co_{17}R$ phase as cells surrounded by $SmCo_5$ boundary with Zr-rich platelet phases running across cells and cell boundaries. $SmCo_5$ phase is responsible for enhancement of coercivity by domain wall pinning mechanism.

An alternative route to fabricate nanostructure, high-temperature magnets is mechanical alloying [4,5]. $SmCo_7$-type nanophase hard magnets with high coercivity and enhanced remanent magnetization were synthesized using mechanically induced amorphization and the crystallization of nanoscaled grains during the subsequent annealing processes. Optimal coercivity of 2.1 T and remanent magnetization of 0.77 T have been obtained in $Sm_{12.5}Co_{85.5}Zr_2$ magnet [6].

Besides mechanical alloying, melt spinning has been proved to be another effective route to fabricate nanocomposite permanent magnets, especially in the Nd−Fe−B system. To obtain nanocrystalline microstructure and high coercivity, it is necessary to make amorphous ribbons first and then crystallize them by annealing. Unfortunately, the amorphous formation ability of Sm−Co alloys is very poor [7]. Thus, the fine microstructure for high coercivity is difficult to realize in melt spun ribbons. However, it has been shown that a small amount of carbon addition is helpful for the grain refinement in the systems of Sm−Co−Hf−C [8], Sm−Co−Nb−C [9], and Sm−Co−Fe−C [10]. Recently, the effects of the addition of Cr_3C_2 on the magnetic properties and microstructure of $SmCo_7$-type magnets have been investigated. It has been found that, even melt-spinning at a low wheel surface speed of 20 m/s, the grain size of Cr_3C_2-doped $SmCo_7$ alloys is significantly reduced from 300−600 nm to below 80 nm [11]. In the present work, the effect of Cr_3C_2 content and wheel speed on the amorphization behavior of the melt-spun $SmCo_{7-x}(Cr_3C_2)_x$ alloys was studied.

2 Experimental

Alloys with nominal compositions of $SmCo_{7-x}(Cr_3C_2)_x$ (x=0.10−0.25) were prepared by arc

Foundation item: Project (51104188) supported by the National Natural Science Foundation for Young Scholars of China
Corresponding author: LI Li-ya; Tel: +86-731-88877328; E-mail: liliya@csu.edu.cn
DOI: 10.1016/S1003-6326(11)61292-2

melting under high purity argon atmosphere. Samples were remelted to ensure homogeneity and an excess of 7% Sm was added to compensate for the Sm loss during processing. The arc-melted ingots were cut into small pieces and then were melt-spun at 20, 30 and 40 m/s. The as-spun ribbons were sealed in quartz tube under vacuum and then annealed at 650−800 °C for 5 min to crystallize and develop a fine microstructure. The crystal structure of the ribbons was identified by Bruker D8 Advance/Discover X-ray diffraction (XRD) system with Phillips diffractometer using the Co K_α radiation. The phase transformation temperatures were determined by differential scanning calorimeter (DSC) at a heating rate of 40 K/min. Hard magnetic properties at room temperature were measured by a Lake Shore 7410 vibrating sample magnetometer (VSM) with the maximum field of 2.3 T. The magnetization of the ribbons could not be saturated using VSM, therefore the maximum magnetization M^{2T} under 2 T was used to represent the saturation magnetization M_s.

3 Results and discussion

3.1 Effects of Cr_3C_2 content and wheel speed on structure of $SmCo_{7-x}(Cr_3C_2)_x$ alloys

The progress of the amorphization process by melt spinning can be seen through the measurement of relative intensity of the XRD patterns of $SmCo_7$-type phase. Figure 1 shows the XRD patterns for $SmCo_{7-x}(Cr_3C_2)_x$ (x=0.10−0.25) ribbons spun at 20 m/s. It can be seen that $SmCo_7$ main phase coexists with $Sm_2Co_{17}R$ secondary phase, which is confirmed by the supperlattice reflection peak of (015), for the series of ribbons. Meanwhile, with increasing Cr_3C_2 content x from 0.10 to 0.25, the intensity of XRD peaks comes to be significantly weaker and the peak width becomes broader, indicating a dramatic decrease in the grain size of the $SmCo_7$ phase. Interestingly, the formation of crystallographic texture is also observed from the XRD patterns. The intensity of diffraction (002) for the $SmCo_7$ phase is strengthened significantly with Cr_3C_2 content x increased to higher than 0.1. This is similar to that observed in $SmCo_7Ti$ and $SmCo_5$ alloys melt-spun at much lower wheel surface speed of 10−15 m/s. In the $SmCo_7$- or $SmCo_5$- type magnets, the intensity of (002) plane is considered measure of texture [12]. This texture is thought to be helpful for the fabrication of anisotropic permanent magnetic materials.

The XRD patterns for $SmCo_{7-x}(Cr_3C_2)_x$ (x=0.10−0.25) ribbons melt-spun at 30 m/s are shown in Fig. 2. It is found that only the $SmCo_7$ phase exists for the ribbon with x=0.10. Two phases, $SmCo_7$ and Sm_2Co_{17}, are detected for ribbons with a higher Cr_3C_2 substitution. A similar dependence of the intensity of XRD peaks on Cr_3C_2 content is observed. It can be found that, with the increase of Cr_3C_2 content, the XRD peaks become significantly low and accompanied with a broad increase in backgrounds, indicating a considerable decrease in the grain size of the $SmCo_7$ phase. The intensity of diffraction (002) for the $SmCo_7$ phase is also gradually strengthened when Cr_3C_2 content x increases from 0.10 to 0.25. For the ribbon with x=0.20, the intensity ratio $I_{(002)}/I_{(111)}$ is 4.04 which is much higher than 3.2 for $SmCo_7Ti$ and 2.9 for $SmCo_5$ magnets [12]. This indicates that the addition of Cr_3C_2 may favor the alignment of $SmCo_7$ crystalline grains during melt spinning. Further investigations are needed to understand this point.

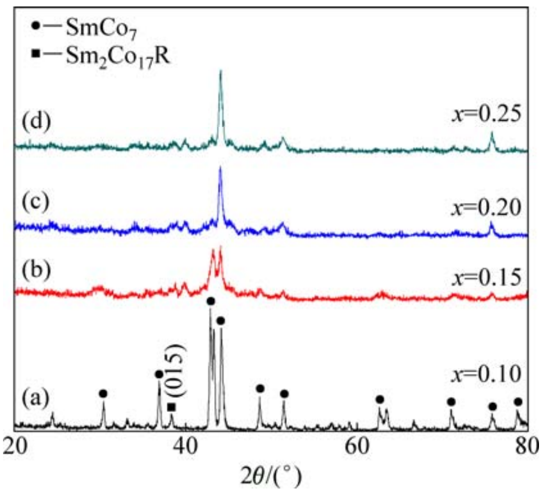

Fig. 1 XRD patterns for $SmCo_{7-x}(Cr_3C_2)_x$ (x=0.10–0.25) alloys melt-spun at 20 m/s

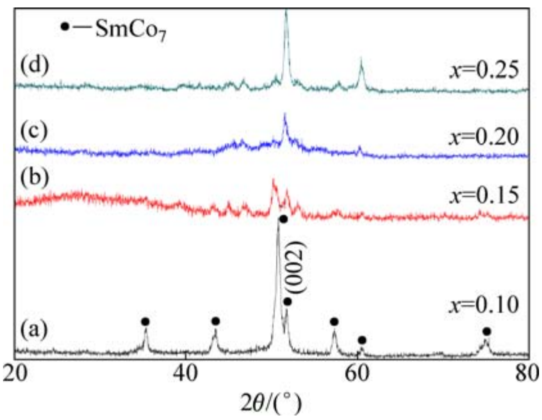

Fig. 2 XRD patterns for $SmCo_{7-x}(Cr_3C_2)_x$ (x=0.10–0.25) alloys melt-spun at 30 m/s

Figure 3 shows the XRD patterns of $SmCo_{7-x}(Cr_3C_2)_x$ ribbons melt-spun at 40 m/s as a function of Cr_3C_2 content. It can be seen that the peaks are found to be broadened and the intensities become significantly low with the increase of wheel surface speed to 40 m/s, indicating that the alloy is driven towards amorphous structure. For the alloys with $x\geq0.15$, the crystalline structure disappears completely and an amorphous-type phase is developed progressively in the alloys.

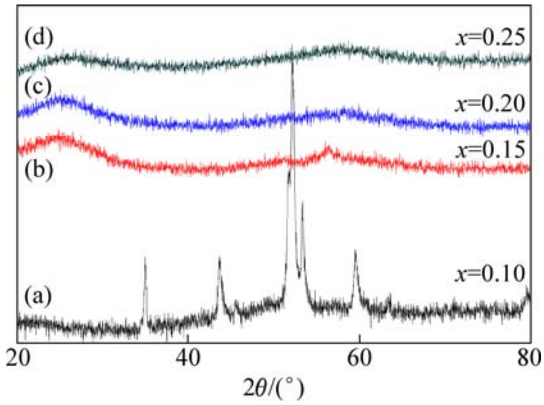

Fig. 3 XRD patterns for $SmCo_{7-x}(Cr_3C_2)_x$ (x=0.10–0.25) alloys melt-spun at 40 m/s

3.2 Magnetic properties

Hysteresis loops of the alloys melt-spun at 30 m/s are shown in Fig. 4. A systematic change in the shape of the loop with the addition of Cr_3C_2 can be seen and the magnetic properties evaluated from these loops are listed in Table 1. With increasing Cr_3C_2 content x, the remanence M_r of the alloys increases up to the maximum value of 0.61 T at x=0.20, beyond which it then decreases to 0.16 T at x=0.25. Meanwhile, the remanence ratio (M_r:M^{2T}) of the alloy increases from 0.67 at x=0.10 to 0.76 at x=0.20, and then decreases to 0.34 at x=0.25. The M_r increases with increasing Cr_3C_2 content, which is likely attributed to the stronger inter-grain exchange coupling between $SmCo_7$ phases due to the finer grain size as observed in the broadened XRD patterns. On the other hand, the coercivity H_{ci} initially increases from

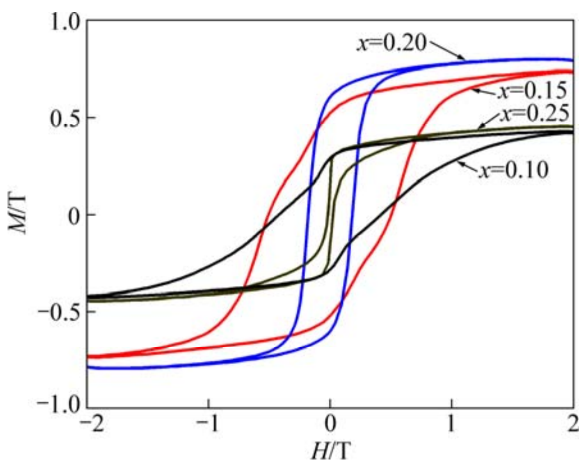

Fig. 4 Hysteresis loops of $SmCo_{7-x}(Cr_3C_2)_x$ (x=0.10–0.25) melt-spun at 30 m/s

Table 1 Magnetic properties of $SmCo_{7-x}(Cr_3C_2)_x$ (x=0.10–0.25) melt-spun at 30 m/s

x	H_{ci}/T	M_r/T	M^{2T}/T	M_r:M^{2T}
0.10	0.42	0.29	0.43	0.67
0.15	0.50	0.52	0.73	0.71
0.20	0.18	0.61	0.80	0.76
0.25	0.02	0.16	0.45	0.34

0.42 T at x=0.10 to 0.50 T at x=0.15 and thereafter decreases to 0.02 T at x=0.25. This behavior is attributed to size effect of coercivity in fine grain sizes, i.e from multi-domain configuration to superparamagnetic state through single domain size [13]. Another reason for the decrease of coercivity may be ascribed to the formation of minor amorphous phase [14,15]. In magnetization reversal, the amorphous phase can act as reverse domain wall nucleation site and will decrease the coercivity.

Figure 5 corresponds to the hysteresis loops of the alloys melt spun at 40 m/s. Those alloys show soft magnetic behavior with narrow hysteresis loops. The coercivities of the as-spun ribbons with $x\geq0.15$ are found to be very low, ranging from 0.004 T to 0.007 T, and decrease with the increasing of x. A reduction of the amount of $SmCo_7$ crystal phase and the increase of the amorphous phase, as shown in Fig. 3, are responsible for this low coercivity.

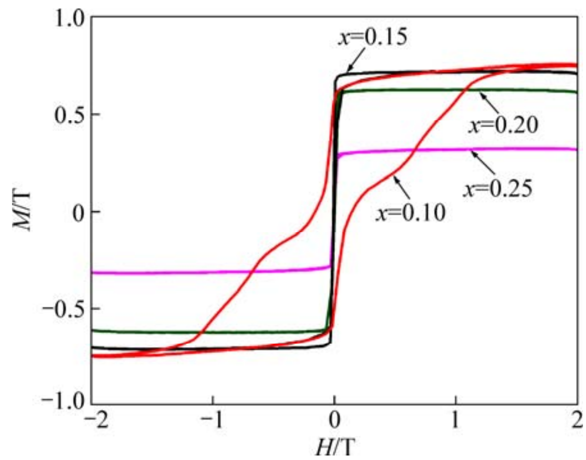

Fig. 5 Hysteresis loops of $SmCo_{7-x}(Cr_3C_2)_x$ (x=0.10–0.25) melt-spun at 40 m/s

3.3 DSC analysis of amorphous structure

Figure 6 presents the DSC curves for crystallization of amorphous $SmCo_{6.75}(Cr_3C_2)_{0.25}$ and $SmCo_{6.80}(Cr_3C_2)_{0.20}$ ribbons. There are two exothermic peaks in both crystallization curves. The first exothermic peak (650 °C) can be attributed to the formation of $SmCo_7$ phase initially from the amorphous phase, and the second one (770 °C) is related to the formation of Sm_2Co_{17} phase. Therefore, the crystallization behavior of this $SmCo_7$ alloy doped with Cr_3C_2 is that $SmCo_7$ phase first precipitates from the amorphous matrix at 650 °C, followed by the crystallization of Sm_2Co_{17} phase at 770 °C. It should also be noticed that the crystallization behaviors of the two alloys with different Cr_3C_2 contents are distinctly similar.

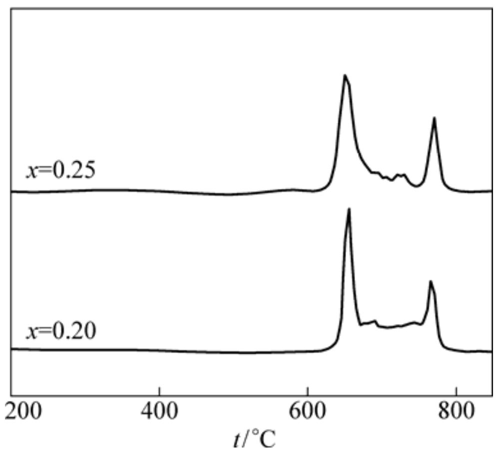

Fig. 6 DSC curves of melt-spun $SmCo_{7-x}(Cr_3C_2)_x$ (x=0.20, 0.25) glassy alloy ribbons

4 Conclusions

1) $SmCo_{7-x}(Cr_3C_2)_x$ ribbons melt-spun at 20 m/s have composite structure composed of main $SmCo_7$ and a small amount of $Sm_2Co_{17}R$ phase. The grain size of $SmCo_7$ phase decreases with increasing the Cr_3C_2 content.

2) With the increase of wheel speed, the XRD peaks of $SmCo_{7-x}(Cr_3C_2)_x$ alloys become significantly low and accompanied with a broad increase in backgrounds, indicating a considerable decrease in the grain size of the $SmCo_7$ phase. The ribbons melt-spun at 40 m/s exhibit amorphous structure in the range of $0.15 \le x \le 0.25$.

3) In the amorphous state, $SmCo_{7-x}(Cr_3C_2)_x$ ($0.15 \le x \le 0.25$) alloys are soft magnetic with intrinsic coercive of 0.004−0.007 T. The DSC analysis reveals that $SmCo_7$ phase firstly precipitates from the amorphous matrix at 650 °C, followed by the crystallization of Sm_2Co_{17} phase at 770 °C. It also can be drawn that the addition of Cr_3C_2 favors the high degree of alignment of $SmCo_7$ crystalline grains during melt spinning.

References

[1] LI Li-ya, YI Jian-hong, GE Yi-cheng, PENG Yuan-dong. Microstructure and coercivity mechanism of Sm_2Co_{17} type high temperature rare-earth permanent magnets [J]. Transactions of Nonferrous Metals Society of China, 2008, 18(1): 72−77. (in Chinese)

[2] HSIAO A, AICH S, LEWIS L H, SHIELD J E. Magnetization processes in melt-spun Sm−Co-based alloys with the $TbCu_7$-type structure [J]. IEEE Trans Magn, 2004, 40(4): 2913−2916.

[3] LIU J F, DING Y, ZHANG Y, DIMITAR D, ZHANG F, HADJIPANAYIS G C. New rare-earth permanent magnets with an intrinsic coercivity of 10 kOe at 500 °C [J]. J Appl Phys, 1999, 85(8): 5660−5662.

[4] GALLAGHER K, GOUIL A L, VENKATESAN M, COEY J M D. Structure and magnetic properties of mechanically alloyed SmZr(Co,Fe) nanophase hard magnets [J]. IEEE Trans Magn, 2002, 38(5): 2916−2918.

[5] GOPALAN R, SURESH K, SRIDHARA RAO D V, SINGH A K, RAMA RAO N V, BHIKSHAMAIAH G, CHANDRASEKARAN V. Amorphization, nanocrystallization and magnetic properties of mechanically milled Sm−Co magnetic powders [J]. Int J Mater Res, 2008, 99(7): 773−780.

[6] TANG H, LIU Y, SELLMYER D J. Nanocrystalline $Sm_{12.5}(Co,Zr)_{87.5}$ magnets: Synthesis and magnetic properties [J]. J Magn Magn Mater, 2002, 241(2−3): 345−356.

[7] PAN Jing, LIU Xin-cai, GUO Peng-ju, XIAO Jun, XU Feng. Crystalline texture and magnetic anisotropy of $Sm(CoFeCuZr)_{12}$ melt-spun ribbons [J]. The Chinese Journal of Nonferrous Metals, 2008, 18(11): 2020−2024. (in Chinese)

[8] CHANG H W, CHEN I W, CHANG C W, FANG Y K, HSIEH C C, CHANG W C, SUN A C, YAO Y D. Magnetic properties, phase evolution, and microstructure of melt-spun $(Sm_{1-x}Pr_x)Co_{7-y}Hf_yC_z$ (x=0−1; y=0.1−0.3; z=0−0.14) ribbons [J]. J Appl Phys, 2008, 103 (7): 07E112.

[9] AICH S, SHIELD J E. Effect of Nb and C additives on the microstructures and magnetic properties of rapidly solidified Sm−Co alloys [J]. J Alloy Compd, 2006, 425(1−2): 416−423.

[10] SULTANA D, GABAY A M, HADJIPANAYIS G C. High performance isotropic Sm−(Co,Fe)−C and Sm−(Co,Fe,Mn)−C magnets by melt spinning [J]. J Appl Phys, 2008, 103 (7): 07E125.

[11] LI L Y, YAN A, YI J H, ZHANG G T, XIE W, SUN Y L, JIE C R, LU H M. Phase transformation, grain refinement and magnetic properties in melt-spun $SmCo_{7-x}(Cr_3C_2)_x$ (x=0−0.25) ribbons [J]. J Alloy Compd, 2009, 479(1−2): 78−81.

[12] SARAVANAN P, GOPALAN R, PRIYA R, GHOSAL P, CHANDRASEKARAN V. Textured resin-bonded $Sm(Co, Fe, Cu)_5$ nanostructured magnets exploiting magnetic field and surfactant-assisted milling [J]. J Alloy Compd, 2009, 477(1−2): 322−327.

[13] HADJIPANAYIS G C. Nanophase hard magnets [J]. J Magn Magn Mater, 1999, 200(1−3): 373−391.

[14] YAN X, SONG X, LI E, WANG J, ZHANG J. Preparation and characterization of binary Sm−Co bulk amorphous alloy [J]. Rare Metal Materials and Engineering, 2008, 37(4): 730−732.

[15] RAJASEKHAR M, AKHTAR D, MANIVEL RAJA M, RAM S, CHANDRASEKARAN V. Structure and magnetic properties of $Nd_{4.5}Fe_{77-x}Sn_xB_{18.5}$ nanocomposite alloys [J]. J Phys D: Appl Phys, 2009, 42: 095009−095016.

Cr_3C_2 含量和快淬速度对 $SmCo_{7-x}(Cr_3C_2)_x$ 合金非晶化行为的影响

李丽娅，易健宏，李爱坤，彭元东，夏庆林

中南大学 粉末冶金国家重点实验室，长沙 410083

摘　要：通过 X 射线衍射法(XRD)、差示扫描量热法(DSC)和磁性测量等方法系统研究 Cr_3C_2 含量和快淬速度对 $SmCo_{7-x}(Cr_3C_2)_x$(x=0.10−0.25)非晶化行为的影响。结果表明，在低的快淬速度下(20 m/s)下，合金主要由 $SmCo_7$ 主相和少量 $Sm_2Co_{17}R$ 相构成，且 $SmCo_7$ 相的晶粒尺寸随着 Cr_3C_2 含量 x 的增加而减小。随着快淬速度的增加，合金的 XRD 衍射峰强度变弱、衍射峰宽化，表明 $SmCo_7$ 主相的晶粒尺寸随着快淬速度的增加而减小。当快淬速度增加至 40 m/s 时，$SmCo_{7-x}(Cr_3C_2)_x$($0.15\le x\le 0.25$)合金均形成了非晶态结构，合金的磁滞回线表现为软磁性的窄回线，矫顽力为 0.004~0.007 T。采用 DSC 对合金的晶化行为分析表明，在 650 °C 时 $SmCo_7$ 相首先从非晶基体中析出，在 770 °C 时 Sm_2Co_{17} 相析出。

关键词：$SmCo_7$ 型永磁材料；Cr_3C_2；快淬；非晶化；磁滞回线

(Edited by LI Xiang-qun)